The Journal of Chemical Physics

# Microrheology of a thermosensitive gelling polymer for cell culture

Cite as: J. Chem. Phys. **157**, 174901 (2022); https://doi.org/10.1063/5.0086533
Submitted: 26 January 2022 • Accepted: 19 May 2022 • Accepted Manuscript Online: 19 May 2022 • Published Online: 07 November 2022

Stefano Buzzaccaro, Vincenzo Ruzzi, Tommaso Faleo, et al.







AIP Publishing

The Journal of Chemical Physics ARTICLE scitation.org/journal/jcp

# Microrheology of a thermosensitive gelling polymer for cell culture

Cite as: J. Chem. Phys. 157, 174901 (2022); doi: 10.1063/5.0086533
Submitted: 26 January 2022 • Accepted: 19 May 2022 •
Published Online: 7 November 2022



Stefano Buzzaccaro,[a] Vincenzo Ruzzi, Tommaso Faleo, and Roberto Piazza

## AFFILIATIONS

Department of Chemistry, Materials Science, and Chemical Engineering (CMIC), Politecnico di Milano, Edificio 6, Piazza Leonardo da Vinci 32, 20133 Milano, Italy

**Note:** This paper is part of the JCP Special Topic on Slow Dynamics.
[a]**Author to whom correspondence should be addressed:** stefano.buzzaccaro@polimi.it

## ABSTRACT

We investigate the rheo-mechanical properties of Mebiol Gel®, a thermosensitive gel-forming polymer extensively used as a medium for cellular culture, using passive microrheology made either by standard dynamic light scattering or by photon correlation imaging. In the dilute limit, Mebiol displays a Newtonian behavior with an effective viscosity that decreases with temperature, consistent with a peculiar aggregation mechanism characterized by an increase of the molecular weight with a simultaneous *reduction* of the aggregate size. By increasing concentration and approaching gelation, both the storage and loss moduli show a nonmonotonic dependence with temperature, with a pronounced maximum around $T_m \simeq 28$–$30\,^{\circ}\mathrm{C}$, the value above which, in the dilute limit, the individual Mebiol chains are fully compacted. Such a distinctive trend of the elastic and viscous properties persists within the gel, which, therefore, becomes "softer" above $T_m$. Although when temperature changes are performed adiabatically, the transition from the fluid to the gel phase takes place without any apparent discontinuity, a rapid $T$-jump leads to the formation of a hard gel at a concentration where a low heating rate conversely yields a fluid phase. This is a visible manifestation of the nonequilibrium nature of these physical gels.



## I. INTRODUCTION

Physical gels, characterized by cross-links with a finite lifetime, have recently aroused interest as suitable candidates for 3D cell growth because of their distinctive propensity to restructuring either spontaneously or under weak stress,[1,2] which allows cells to grow, multiply, and migrate. Among several options, a special role is taken by thermoreversible polymer gels reverting to a low-viscosity fluid at moderately low temperature, both because cell seeding and recovery are much easier in a liquid phase and since the rheo-mechanical properties of these gels can easily and accurately be tuned by varying temperature.

A promising strategy to obtain thermoreversible gels exploits high molecular weight copolymers composed of blocks of polyethylene glycol (PEG) randomly intermixed with blocks of poly(*N*-isopropylacrylamide-co-*n*-butylmethacrylate) [poly(NIPAAm-co-BMA)]. The latter retain the distinctive property of poly(*N*-isopropylacrylamide) (PNIPAm), showing a decreasing solubility in water with increasing $T$ that eventually leads to phase separation.[3,4] Yet, this demixing process is fully quenched for the random block copolymer because of the strongly hydrophilic character of the PEG blocks. Nevertheless, at sufficiently high $T$ and moderately high concentration, aqueous solutions of these block copolymers undergo a thermoreversible sol–gel transition, arguably due to hydrophobic interactions between poly(NIPAAm-co-BMA) blocks leading to the formation of interchain cross-links. Careful engineering of the composition of these block copolymers has led to a patented material, commercially known as Mebiol Gel®, whose mechanical strength and permeability at physiological temperature are highly suitable for cell growth and differentiation,[5] which has proved to enable regeneration of damaged tissues *in vivo*.[6,7]

Besides its importance in applications, Mebiol provides an interesting system to investigate gelation in block copolymer solutions. In particle suspensions, there are just two well-defined routes to gelation.[8] Videlicet, while gelation is always associated with the kinetic arrest of a phase separation process for colloidal particles with isotropic interactions, "patchy" particles with a limited valence can gel following an equilibrium pathway. While colloidal

gels generated by arrested phase separation are usually spatially heterogeneous and display an intermittent aging dynamics characterized by sudden local and global structural rearrangements, equilibrium gels are predicted to be much more spatially uniform and temporally stable. Such a contrasting behavior has recently been observed in solution of tetravalent DNA nanostars that, depending on the particle concentration, can form either equilibrium or kinetically arrested gels.[9] The detailed conditions for gelation in copolymer systems induced by the presence of "sticking" blocks are still partly understood.[10] Indeed, whether these blocks generate inter-chain rather than intra-chain cross-links surely depends on the overall chain concentration $c$, with the probability of inter-chain bonds rapidly growing with $c$, but is arguably conditioned by several other factors, such as the molar fraction of sticking blocks, their size, and their distribution along the chain. As a matter of fact, cross-link formation is often a highly cooperative process that can be affected by the way gelation is induced. For instance, sodium alginate gels are strongly heterogeneous when obtained by external perfusion of divalent ions,[11] but are much more uniform when produced by internal enzymatic activation of a curing agent.[12]

Mebiol retains some features of the gelation by arrested phase separation of simple colloids, such as a growth of concentration fluctuations by approaching gelation and within the gel region itself testified by a huge increase of the scattered intensity $I_s$ with temperature. Yet, $I_s$ does not diverge, but rather reaches a plateau value, while in the same temperature range the system correlation length (the network mesh size) displays just a modest change.[13] In other words, the propensity of the poly(NIPAAm-co-BMA) blocks to phase segregate from the solvent is fully frustrated by the presence of the hydrophilic PEG groups. Actually, gelation of this thermosensitive polymer occurs with no apparent discontinuity in the structural and dynamic properties of the solution; hence, a boundary of the gel region can only be roughly defined by appealing to macroscopic tests of the mechanical rigidity. By approaching this region, however, the correlation functions measured by Dynamic Light Scattering (DLS) progressively attain a logarithmic decay, which suggest that gelation actually involves a percolation process.[13] The main purpose of this paper is scrutinizing the microrheology properties of Mebiol solutions in relation to this peculiar gelation process. A further issue that is critically addressed in this work is whether Mebiol gelation can truly be considered an equilibrium process or whether the system rheo-mechanical properties actually depend on the rate of temperature increase.

## II. MATERIALS AND METHODS

### A. Sample composition and preparation

Mebiol (Cosmo Bio Co., Ltd., Tokyo, Japan) is obtained by reacting suitably activated NIPAAm-co-BMA monomers with diamino-PEG6000 (corresponding to about 230 ethylene glycol monomers). The commercial product has an overall PEG6000 content of about 34% in weight and contains a random and widely polydisperse distribution of thermosensitive poly(NIPAAm-co-BMA) blocks with a molar fraction of BMA of about 5%. The polymer is supplied as a powder in a sterilized flask. Preparation of a mother batch was made by adding 50 ml of ultrapure water to 5 g of the lyophilized polymer and placing the flask in a refrigerator where it was shaken from time to time. The homogeneous solution was further kept at a low temperature for a few days to ensure complete polymer dissolution. This mother batch, at a nominal concentration of 90 g/l, was further diluted in volume with ultrapure water to obtain the samples discussed in the text. A description of the phase behavior and the microscopic dynamics of Mebiol can be found in a recent paper,[13] to which we refer for further details on the sample properties.

Passive microrheology was performed by adding to the samples PMMA particles (Microparticles GmbH), of radius $a = 96$ nm, at fixed concentration equal to 0.02 w/v%. In the investigated temperature range, multiple scattering effects are avoided and the signal coming from the light scattered by the tracer particles is at least one order of magnitude larger than the contribution of the bare polymer solution.

### B. Microrheology

Passive microrheology studies were performed according to the method originally introduced by Mason and Weitz,[14] which consists of adding tracer particles of radius $a$ to the material of interest, obtaining their mean-square displacement (MSD) $\langle \Delta r^2(t) \rangle$ as a function of time from the decay rate of the correlation function of the scattered intensity. The MSD can then be related to the frequency-dependent complex modulus $\tilde{G}(s)$ by using the generalized Stokes–Einstein relation[15]

$$\tilde{G}(s) = \frac{N k_B T}{3\pi a s \langle \Delta r^2(s) \rangle}, \tag{1}$$

where $\langle \Delta r^2(s) \rangle$ is the Laplace transform of the MSD in $N$ dimensions as a function of the complex frequency $s$. For what follows, it is worth pointing out that Eq. (1) strictly holds when the tracers are dispersed in a homogeneous medium, or at least when their size is consistently larger than any local structure of the dispersant.

The real frequency-dependent complex shear modulus $\tilde{G}(\omega) = G'(\omega) + iG''(\omega)$ can then be retrieved by taking the analytical continuation of $\tilde{G}(s)$, imposing $s = i\omega$; the storage and loss moduli are simply the real and imaginary parts of $\tilde{G}(\omega)$, respectively.

Experimentally, the MSD of tracer particles can be extracted from a standard Dynamic Light Scattering (DLS) measurement by observing that, for sufficiently diluted tracers, the intensity time-correlation function is given by

$$g_2(t) = 1 + e^{-q^2 \langle \Delta r_q^2(t) \rangle}, \tag{2}$$

where $\langle \Delta r_q^2(t) \rangle$ is the component of the MSD along the direction of the scattering wave-vector $q$. For a 3D isotropic motion, the total MSD is then given by

$$\langle \Delta r^2(t) \rangle = -\frac{3}{q^2} \ln(g_2(t) - 1). \tag{3}$$

Although, in principle, $\tilde{G}(s)$ can be calculated through Eq. (1) by a numerical Laplace transform of the MSD data, in order to reduce errors near the frequency-range limits, we used the Kilfoil-group

software.[16] The software implements an algebrical inversion procedure based on the work of Mason,[17] which is based on power law approximations of the MSD data and an algebraic approximation to the generalized Stokes–Einstein with second-order logarithmic derivative corrections. When the MSD is purely diffusive, like in a fluid, $G''$ is accurately computed, whereas the estimate for $G'$ is poorer. Conversely, when the MSD tends to saturate, like in an arrested or quasi-arrested phase, $G'$ is correctly estimated, while the values of $G''$ are affected by large uncertainties.[17]

Since the total acquisition time required to obtain an adequate statistics in the correlation function has to be much longer than the typical decay time of the investigated process, standard DLS methods are, however, unsuited for microrheology studies in systems, such as physical gels displaying a slow dynamics. To overcome this limitation, we have used Photon Correlation Imaging (PCI), a recently introduced optical method that measures the time-correlation function of the scattered intensity like DLS, but has the major advantage of being a multispeckle technique allowing for spatial resolution by simultaneously probing the local dynamics at distinct points within the scattering volume. The simultaneous measurement of the time dynamics over many speckles by a multipixel detector provides a fast ensemble averaging of the intensity correlation function, allowing at the same time spatial heterogeneity in the sample microscopic dynamics to be detected. Further details on the PCI technique and on the setup we used, which operates at a fixed scattering angle $\vartheta = 90°$ (corresponding to a wave-vector $q = 23\ \mu m^{-1}$), can be found in the work by Piazza *et al.*[13]

### C. Auxiliary measurements

Subsidiary viscosity measurements at a concentration of $c = 10$ g/l (where Mebiol shows a Newtonian behavior, as discussed below) were performed with a calibrated Ubbelohde microviscometer (Xylem Analytics Germany GmbH, filling volume 3 ml), immersed in a water thermostat (Haake F3) with a window allowing for optical inspection. In this dilute condition, the dynamic viscosity $\eta = \rho\nu$ is obtained from the measured kinematic viscosity $\nu$ by taking the solution density $\rho$ equal to the density of the solvent.

At higher concentrations, where the Mebiol solutions are no more Newtonian, we had to resort to a different method. Hence, the macroscopic viscometry of Mebiol at $c = 50$ g/l presented in Sec. III A 2 was carried out by measuring the settling speed of a steel ball G100 (radius $b = 250\ \mu$m and density $\rho \simeq 8$ g/cm$^3$), which we assume to be approximately related to the fluid steady-shear viscosity by $v_s = 2\Delta\rho g b^2/(9\eta)$ even for viscoelastic fluids.[18] A glass cuvette was filled with the solution and put in a temperature-controlled water bath, and for each temperature, the probe ball was gently inserted in the solution with the help of an Eppendorf micropipette tip partially immersed in the fluid (see Movie M1 in the supplementary material). The settling speed $v_s = h/\Delta t$ is evaluated from the fall $h \simeq 3$ cm of the ball in a time $\Delta t$. In the measured temperature range, $\Delta t$ approximately varies between 0.6 and 3.4 s, corresponding to an "average" shear rate $\dot{\gamma} \simeq v_s/2b$ ranging from 20 to 110 s$^{-1}$, and the steel ball exerts a stress on the solution $\sigma \simeq 22$ Pa. Qualitative observations of the gel obtained by fast temperature jump at $c = 50$ g/l were also made by displacing the bead inside the sample with a magnet (see Sec. III A 4).

## III. RESULTS

### A. Adiabatic heating

If temperature changes are made very slowly, the system shows a reversible behavior. For instance, if we take a measurement at $T_h$, then bring the system at $T_l < T_h$, and finally heat it back to $T_h$ with very low heating/cooling rates, a second measurement taken at $T_h$ yields a DLS or PCI correlation function that is fully like the first one. We carried out this "adiabatic" heating strategy by filling the scattering cell with the investigated sample at a low temperature ($T = 4\,°$C), heating it to the lowest investigated temperature, and keeping it at that temperature for at least 30 min before starting the measurement. The sample is then brought to the next temperature with a heating rate of 0.5 °C/min and again kept at a fixed $T$ for at least 30 min before starting a new measurement. Using this procedure, we have investigated the system micro-rheological properties along several paths, which are shown in Fig. 1 on the phase diagram of the system obtained in the work of Piazza *et al.*[13] We recall that the gel phase boundary of the latter was obtained by progressively raising $T$ until the yield strength $\sigma$ of the system became sufficiently large ($\sigma \gtrsim 50$ Pa) to prevent a tiny magnetic bar from settling when the sample container was turned upside down, at least on a measuring time of 10 min. Microrheology measurements were taken either by DLS (path 1) or by PCI (paths 2–4).

#### 1. Path 1 (low concentration)

At low concentrations ($c \leq 10$ g/l), Mebiol solutions display a rather anomalous trend with temperature.[13] Indeed, a consistent increase of the scattered intensity with $T$, which strongly suggests the

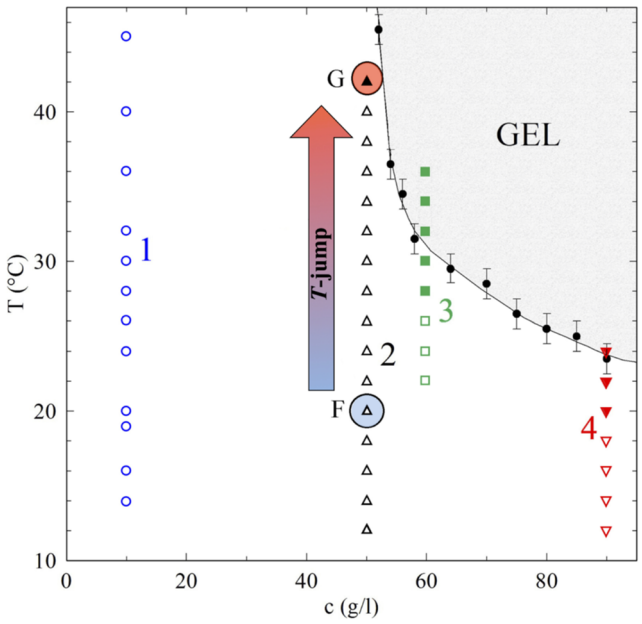


**FIG. 1.** Experimental phase diagram of Mebiol solutions from the work of Piazza *et al.*[13] showing the measurement paths discussed in Sec. III A and the temperature jump from F to G discussed in Sec. III B. Open and full symbols, respectively, refer to "rheologically" fluid ($G'' > G'$) and gelled ($G' > G''$) samples.

formation of aggregates of the individual chains, is not accompanied by a corresponding increase of the hydrodynamic radius obtained by DLS. This has been attributed to the dominant effect of chain compaction leading to a smaller size of an aggregate with respect to that of a unimer even if the molecular weight increases. Such an unexpected effect is actually supported by numerical simulations of a block copolymer system that, albeit much simpler, shares the same basic structure of Mebiol.

It is therefore interesting to investigate if this peculiar association process affects the rheological properties of the solution. We actually found that Mebiol solutions at $c = 10$ g/l display a simple Newtonian behavior over the whole investigated temperature range, as witnessed by the exponential decay DLS field correlation functions by the dispersed particles, $g_1(t) = \exp(-Dq^2t)$, plotted in the inset of Fig. 2. The figure shows that in this temperature range the Mebiol solution viscosity $\eta$, obtained from the diffusion coefficient $D$ of the tracer particles and scaled to the viscosity of water $\eta_0$ at the same temperature, decreases by a factor of about two. Notably, this is very close to the reduction of the average hydrodynamic radius of the Mebiol chains found in the same temperature range.[13]

It is, however, worth pointing out that the average hydrodynamic radius of the polymer coils obtained by DLS[13] increases from about 1/3 to about 3/4 of the PMMA particle radius by decreasing $T$ from 50 to 15 °C. Treating Mebiol solutions as a homogeneous solvent with an effective viscosity $\eta = k_BT/(6\pi aD)$ is, therefore, rather questionable. Actually, Fig. 2 shows that the values found by passive microrheology are higher (up to 25% at low $T$) than those obtained by standard macroscopic measurements. While it is predicted that a nanoprobe experiences a smaller viscosity,[19–21] our result can be easily explained considering an adsorption of the Mebiol chains on the particle surface.[22]

### 2. Path 2 (just before the gel phase)

By increasing the Mebiol concentration, the solution progressively departs from a simple Newtonian behavior. At a concentration of 50 g/l that is far higher than the overlap concentration of the polymer, estimated in about 10 g/l, the decay rate of the correlation functions shown in Fig. 3 displays a pronounced non-monotonic trend with temperature, first slowing down by increasing $T$ but then speeding up for $T \gtrsim 28$ °C.

Figure 3 shows that this behavior can be quantitatively accounted for by fitting the correlation functions as a stretched exponential (SE),

$$g_1(t) = \exp[-(t/\tau)^{\beta}]. \tag{4}$$

This also provides a value for the average decay time of $g_1(\tau)$,

$$\langle\tau\rangle = \int_0^{\infty} g_1(t)dt = \frac{\Gamma(1/\beta)}{\beta}\,\tau, \tag{5}$$

where $\Gamma(x)$ is the gamma function, which is shown in the upper right inset of Fig. 3. Notably, the $T$-dependence of the stretch exponent $\beta$, displayed in the lower left inset, shows that the slower $g_1(t)$ decays, the more its shape deviates from a simple exponential, suggesting that when the Brownian dynamics of tracers is slower, it is also more heterogeneous.

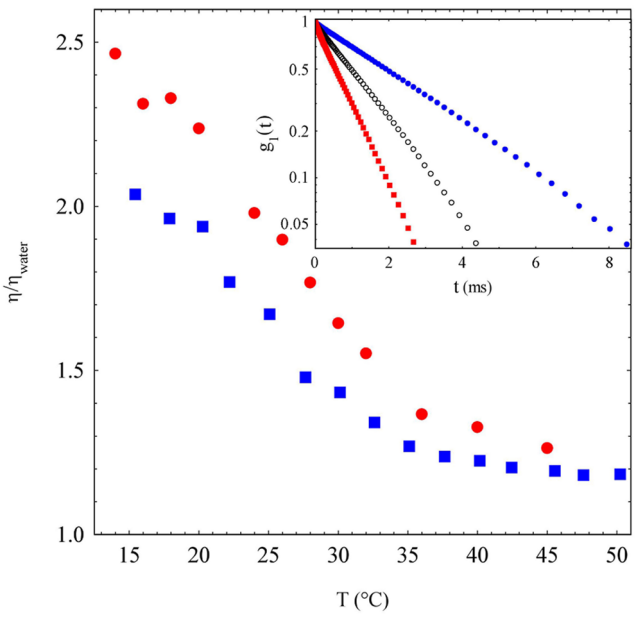


**FIG. 2.** Mebiol viscosity along path 1 ($c = 10$ g/l) normalized to the viscosity of water obtained by microrheology (full circles) and with an Ubbelohde viscometer (squares). Inset: DLS correlation functions at $T = 12$ °C (full circles), $T = 28$ °C (open circles), and $T = 40$ °C (squares).

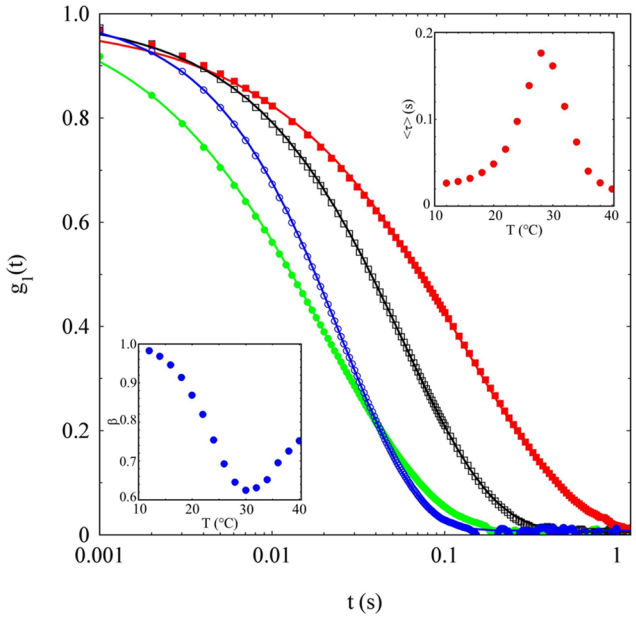


**FIG. 3.** Representative field correlation functions along path 2 at $T = 12$ °C (open dots), $T = 22$ °C (open squares), $T = 30$ °C (full squares), and $T = 38$ °C (full dots). Continuous lines are the fits with a stretched exponential (SE) function $g_1(t) = \exp[-(t/\tau)^{\beta}]$. The two insets show the temperature dependence of the average decay time $\langle\tau\rangle$ and of the stretch exponent $\beta$.

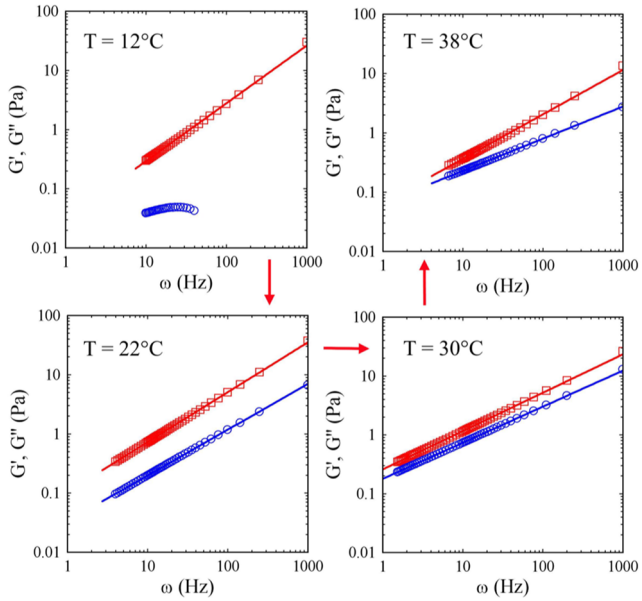


**FIG. 4.** Storage (blue circles) and loss (red squares) moduli along path 2 at four representative temperatures. Full lines are power law fits.

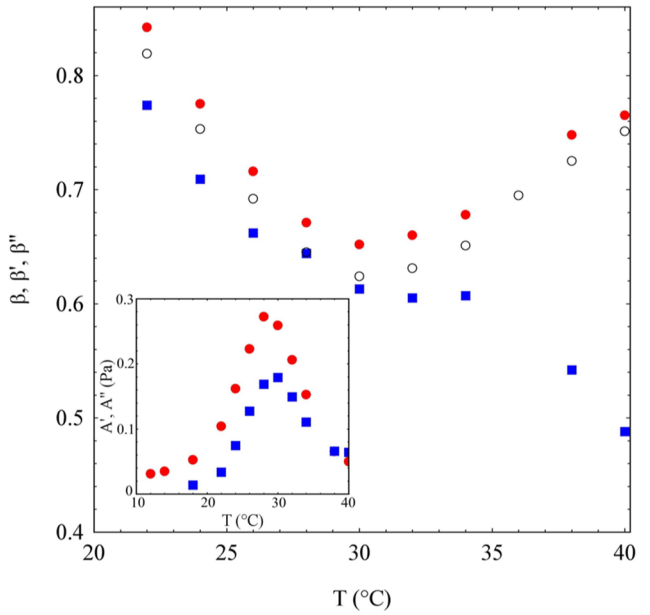


**FIG. 5.** Exponents $\beta'$ (squares) and $\beta''$ (bullets) of the power law fits compared to the stretch exponents $\beta$ shown in Fig. 3 (open circles). The amplitudes of the power law fits to the loss (bullets) and storage (squares) moduli along path 2 are compared in the inset.

Further insights can be obtained by analyzing the correlation functions according to the method introduced by Mason and Weitz.[14] The microrheology results for four representative temperatures, displayed in Fig. 4, show that the loss modulus is larger than the storage modulus for all investigated temperatures and frequencies, indicating that at this concentration the sample never forms what in rheology is regarded as a gel phase. Interestingly, if we exclude the lowest temperatures, where $G'(\omega)$ is too small to be satisfactorily measured, both moduli show a power law behavior,

$$\begin{cases} G' = A' \omega^{\beta'}, \\ G'' = A'' \omega^{\beta''}. \end{cases}$$

The values of the exponents $\beta'$ and $\beta''$ of power law fits to the storage and loss moduli are compared in Fig. 5 to the values of the exponent $\beta$ obtained from the SE fit to the field correlation functions. We note that the values of the exponents $\beta'$ and $\beta''$ are quite close for all investigated temperatures, while $\beta'$ departs from them for $T > 30\,^{\circ}\mathrm{C}$. The fact that $\beta$ and $\beta''$ are comparable is expected because a stretched exponential shape of the intensity correlation function yields a power law behavior of the MSD with the same exponent $\beta$. Since the Laplace transform of a power law is again a power law with the same exponent, we also expect the loss moduli to show an equal trend.

The inset of Fig. 5 shows that the amplitude prefactors of both moduli display a non-monotonic behavior with temperature with maxima around $28\,^{\circ}\mathrm{C}$.[23] Such a non-monotonic behavior of the sample mechanical properties is further appreciated in Fig. 6, where we plot the frequency dependence of the viscosity $\eta(\omega) = \omega^{-1} G''$

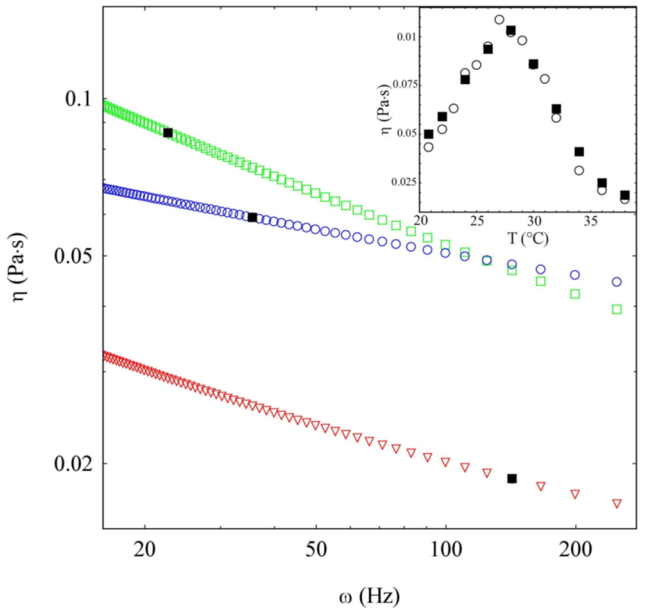


**FIG. 6.** Inset: temperature dependence of the viscosity along path 2 measured by microrheology (squares) or obtained by settling a steel bead (open circles). Main body: viscosity vs frequency for $T = 22\,^{\circ}\mathrm{C}$ (blue circles), $T = 30\,^{\circ}\mathrm{C}$ (green squares), and $T = 38\,^{\circ}\mathrm{C}$ (red triangles). The black squares refer to the values selected at $\omega = \dot{\gamma}$ for the inset plot, as explained in the text.

for three representative temperatures. While the low-frequency viscosity ($\omega < 100$ Hz) rises by heating the sample from $T = 22\,^{\circ}$C to $T = 30\,^{\circ}$C, a further temperature increase to $T = 38\,^{\circ}$C lowers $\eta$ to about half of its value at $T = 22\,^{\circ}$C over the whole investigated frequency range. This peculiar trend is confirmed by the macroscopic viscosity measurements shown in the inset of Fig. 6, where the values of the steady-shear viscosity are compared with the values of the viscosity obtained by microrheology at the frequency $\omega = \dot{\gamma}$. The excellent agreement between the two datasets further validates microrheology as a method to obtain the mechanical properties of Mebiol solutions.

### 3. Path 3 (just inside the gel phase)

Along path 3 ($c = 60$ g/l), the rheological properties of the sample qualitatively change. Except at low $T$, the field correlation functions do not have anymore a SE shape and, for $T > 26\,^{\circ}$C, the storage and loss moduli intersect (see Fig. 7), indicating the onset of a gel phase.[24] Upon a further temperature increase, the range of frequencies where the sample shows a solid-like behavior widens until, for $T \gtrsim 36\,^{\circ}$C, $G'$ becomes larger than $G''$ over the whole frequency range. Nevertheless, the frequency behavior of both $G'(\omega)$ and $G''(\omega)$ departs only slightly from a simple power law. Actually, one can still define a low and high frequency slope of both moduli in the low and high frequency limits whose values, as shown in Fig. 8, are quite close.[25] Figure 8 also shows that, at variance with what we found for the sample at 50 g/l, the values of the $\beta$ exponent at high $\omega$ monotonically decrease with $T$ and level off at $\beta \simeq 0.4$ for $T > 28\,^{\circ}$C. However, the amplitudes of $G'$ and $G''$, shown in the figure inset, still display a non-monotonic trend with $T$. Hence,

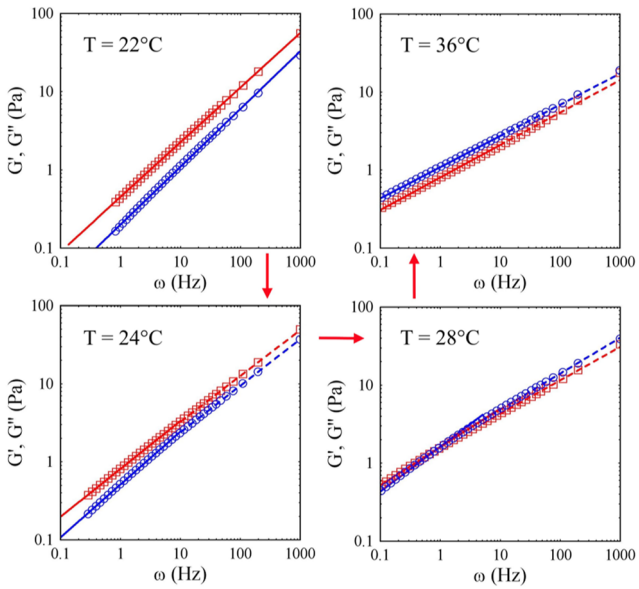


**FIG. 7.** Storage (blue circles) and loss (red squares) moduli along path 3 at four representative temperatures. The dashed lines are power law fittings in the low (high) frequency regions.

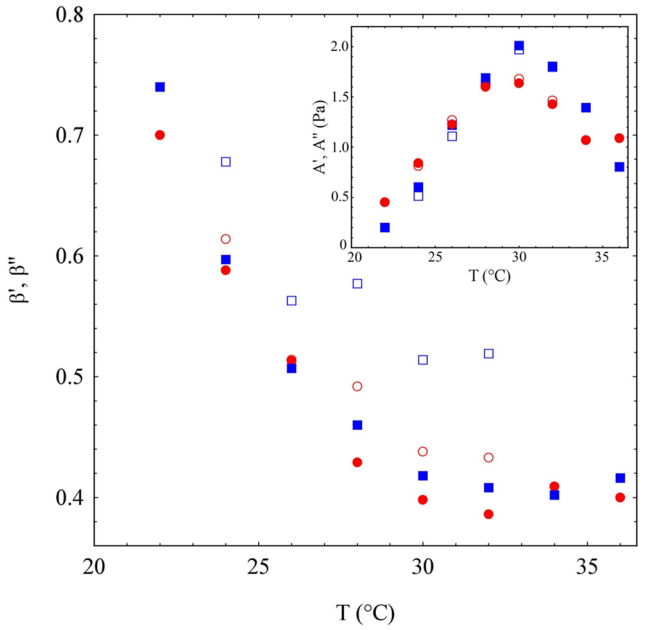


**FIG. 8.** Values of the $\beta'$ and $\beta''$ exponents of the power law fits for the high frequency (full symbols) and low frequency (open symbols) of the loss (circles) and storage (squares) moduli in Fig. 7. The moduli amplitudes are shown in the inset with the same symbols.

although the system becomes rheologically more solid-like by increasing $T$, for $T > 28\,^{\circ}$C, the gel progressively weakens, displaying a behavior that resembles the viscosity decrease observed along path 2. This result is qualitatively confirmed by observing that the settling velocity of the steel ball, used to obtain the macroscopic viscosity along path 2 displayed in Fig. 6, is minimal at $T = 30\,^{\circ}$C. The fact that the ball eventually settles indicates that the yield stress in our gelled samples, if present, is less than 22 Pa.

### 4. Path 4 (well inside the gel phase)

Along path 4, which corresponds to the concentration $c = 90$ g/l suggested by the producer for cell culturing, the system enters the gel phase as soon as $T \simeq 20\,^{\circ}$C, and the frequency region where $G' > G''$ widens by increasing $T$. Unfortunately, by further quenching into the gel region, the scattering contribution due to the polymer solution soon becomes comparable to that due to the tracers, so we had to limit our measurements to a maximum temperature of about of $24\,^{\circ}$C: Besides, even in the limited $T$-range, we managed to investigate the storage and loss moduli cannot be easily fitted by any simple functional form (see Fig. 9), and thus, we just qualitatively observe that the overall dynamics of the sample slows down monotonically and that the gel becomes stronger with $T$. Although it may still be possible that the gel weakens at higher $T$, like we found at lower $c$, the limited macro-rheology results published by the Mebiol producer suggest that the loss and storage moduli monotonically increase with $T$, at least at a very low frequency.

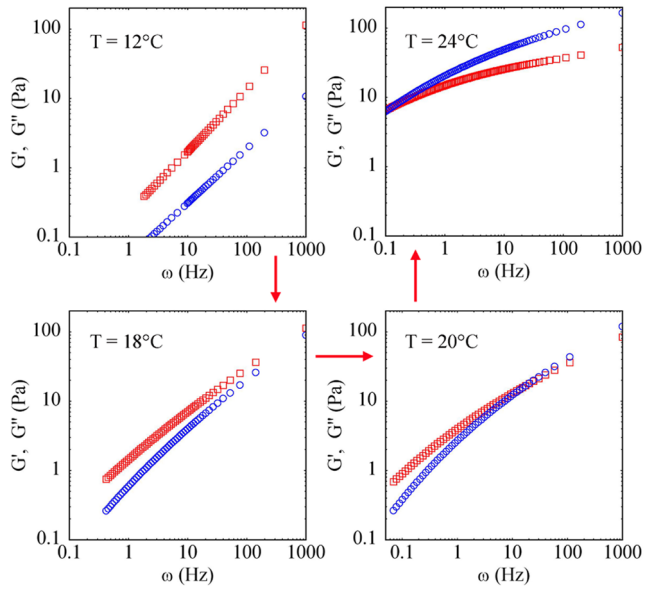


**FIG. 9.** Storage (blue circles) and loss (red squares) moduli along path 4 at four representative temperatures.

### B. Rapid heating (*T*-jump from *F* → *G*)

While, at low concentrations, the system properties do not appreciably depend on the heating rate, the situation remarkably changes for $c \gtrsim 40$ g/l, and the sample rheological properties start to depend heavily on its thermal history. Thermal history effects are particularly striking when we consider the behavior of a sample at $c = 50$ g/l, a concentration value that borders the gel region in Fig. 1. As previously discussed, when heated adiabatically, the system remains in a fluid phase all along path 2. Conversely, a fast $T$-jump made by quickly inserting a sample kept at $T = 20\,^{\circ}$C in the cell holder of the PCI setup, already thermostated at $42\,^{\circ}$C, suddenly leads to the formation of a gel that a simple test made by turning upside down the cell shows to be quite stiff.

In fact, as shown in Fig. 10, the tracer dynamics in this gel is drastically different from that observed in a sample adiabatically brought to the same temperature. While for adiabatic quenching the correlation function can be fitted by a SE with an exponent $\beta \simeq 0.6$ and a decay time $\langle\tau\rangle \simeq 20$ ms, the $T$-jump leads to a correlation function that decays almost *logarithmically* over three to four decades in time (Fig. 11).

Such a huge difference in the microscopic tracer dynamics visibly reflects in the behavior of the storage and loss moduli, as shown in Fig. 11. While for adiabatic heating we recover the power law behavior found along path 2, with $G'$ smaller than $G''$ over the whole frequency range, after the $T$-jump both $G'$ and $G''$ are much larger, with $G'$ *larger* than $G''$ for all values of $\omega$. Besides, while the loss modulus is still approximately a power law with exponent $\beta \simeq 0.4$, the storage modulus approaches for $\omega \to 0$ a constant value of the order of 4–5 Pa, suggesting that the gel generated by the fast quench displays a finite yield stress. This evidence is further supported by observing that, in 10 min, the steel ball used to obtain the

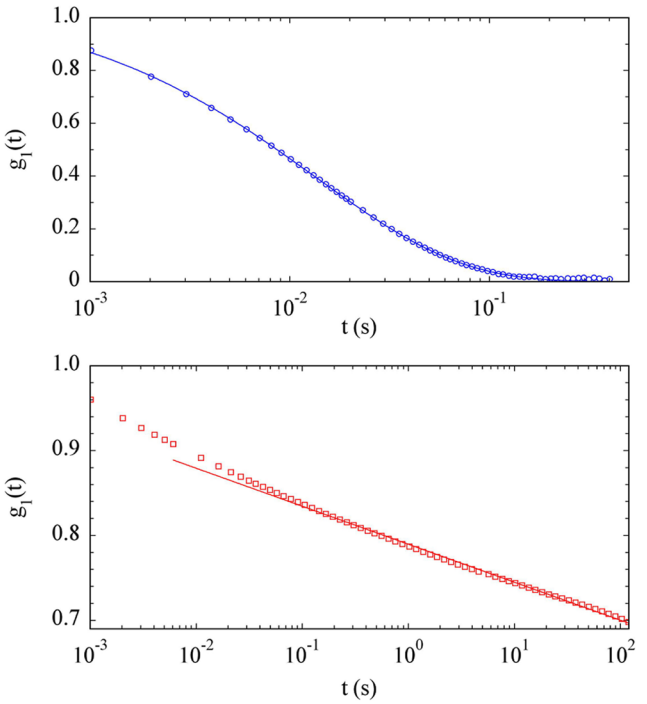


**FIG. 10.** Comparison of the PCI correlation functions for a sample at $c = 50$ g/l adiabatically brought to $42\,^{\circ}$C (top panel), fitted with a stretched exponential (full line) with that of a gel obtained by a fast $T$-jump to the same temperature (bottom panel), where an extended logarithmic decay region is clearly visible. Note the hugely different time scales over which the two correlation functions develop.

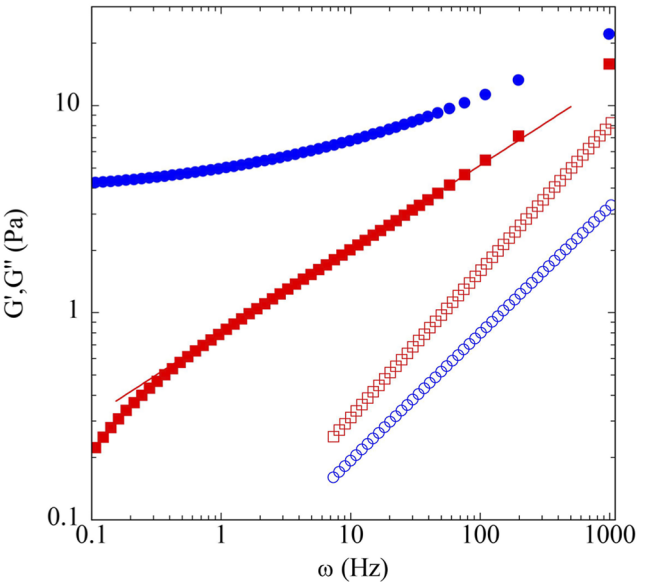


**FIG. 11.** Comparison of the storage (circles) and loss (squares) moduli at $T = 42\,^{\circ}$C, upon adiabatic (open symbols) and rapid (full symbols) heating from $T = 20\,^{\circ}$C.

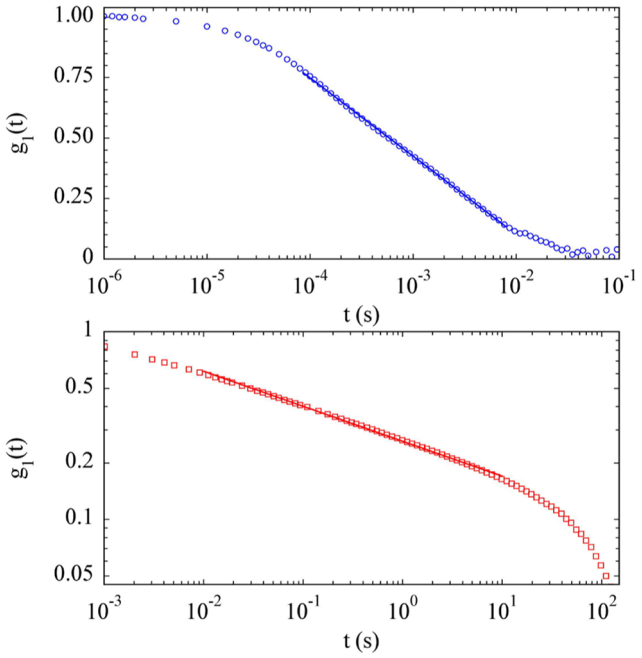


**FIG. 12.** Comparison of the field correlation functions for a pure Mebiol solution at $c = 50$ g/l adiabatically brought to 42 °C (top panel) with that of a gel obtained by a fast $T$-jump to the same temperature (bottom panel). While the former displays an extended logarithmic decay region, in agreement with previous results,[13] over more than four decades in time the latter decays as a power law. Note again the wide difference of time scales between the two graphs.

macroscopic viscosity along path 2 displayed in Fig. 6 does not settle appreciably in the quenched gel. Furthermore, if we try and slightly displace the particle with a magnet, the sample clearly shows an elastic behavior because when the magnetic field is removed the particle comes back to, or close to, its initial position (see Movie M2 in the supplementary material). It is finally useful to investigate whether such a drastic contrast in the rheological properties reflects in the microscopic dynamics of the Mebiol polymer matrix itself, namely, in the absence of tracer particles. Figure 12 shows that the correlation function of the fluid phase obtained by adiabatic heating decays logarithmically over a wide time window, in full agreement with previous results (see Fig. 8 in Ref. 13). Conversely, over about four decades in time, the correlation function of the quenched gel decays as a power law $g(t) \propto t^{\alpha}$, with $\alpha \simeq 0.2$. Once again, the time window for the decay of $g_1(t)$ is orders of magnitude wider in the gel than in the fluid.

## IV. DISCUSSION

Our microrheology results show that in the dilute limit Mebiol solutions behave as simple Newtonian fluids with a viscosity that decreases with temperature, first roughly linearly and then progressively attaining a lower plateau value for $T \gtrsim 30$ °C. This behavior is fully consistent with a previously suggested and rather surprising picture[13] in which the association of the polymer chains due to the increasing "stickiness" of the poly(NIPAAm-co-BMA) blocks does not lead to clusters larger than the individual, non-collapsed chains. Hence, at low $T$, the effective volume fraction occupied by the polymer is actually larger than at higher $T$ where the system is made of compact chain oligomers, which consequently leads to a consistent decrease of the solution viscosity with temperature. It is also rather surprising that an effective-medium approximation to such a structured solvent still reasonably holds even when the sizes of the chains and of the tracers are comparable, in particular, if we allow for a surface adsorption of Mebiol on the PMMA particles.

Along path 2, corresponding to a concentration well above $c^*$ but still in the "mechanically" fluid phase, two conflicting effects take place by slowly raising $T$. On the one hand, the coils tend to form compact aggregates that speed up the dynamics, like in the dilute limit. On the other, however, the formation of transient interchain cross-links, whose strength increases with T, plays an opposite role. Notably, this "tug-of-war" between two opposite tendencies leads to a nonmonotonic $T$-behavior of both the loss and storage moduli,[26–28] both attaining a maximum around the temperature $T \simeq 28$–$30$ °C where the average hydrodynamic radius of the individual chains reaches its lower value.[13] At the same time, this is also the temperature where the exponent of the SE fit to the correlation functions attains a minimum value $\beta \simeq 0.6$, namely, the microscopic dynamics displays the widest distribution of relaxation times. This temporal heterogeneity could arise from a structural hierarchy of time scales experienced by a single probe particle or/and from the occurrence of spatial heterogeneity in the gel. To unravel the origin of this wide distribution of relaxation times, however, further experimental evidence will be required.

At higher concentrations, the interchain cross-links grow in number and strength to the point that the system forms a physical gel. Nevertheless, the moduli still show a similar nonmonotonic behavior with $T$. The main difference between path 2 and path 3, however, is that along the latter the $\beta$ exponents reach consistently lower values, saturating at high $T$ at $\beta \simeq 0.4$.

The general picture stemming from the experiments performed with a very low heating rate is that the fluid/gel transition is continuous, namely, a sharp boundary for the gel region does not really exist and can be stated only by fixing a value for the stress the system can yield over a given time window. Besides, this boundary does not coincide at all with what one would guess from the criterion $G' > G''$ conventionally used in rheology to define a gel phase.

Finally, $T$-jump experiments show that the fully reversible behavior we observed with adiabatic heating/cooling does not imply at all that the system phase behavior is an equilibrium one. The fact that the gel boundary depends on the heating rate is actually consistent with a simple model of competition between chain compaction and increase of the cross-link strength. Indeed, the previously collected evidence[13] suggests that, upon heating, Mebiol solutions take quite a long time to attain a steady-state structure. Hence, if the heating rate is much faster than this intrinsic restructuring time, the chains, already fully entangled at low $T$, remain frozen in a network having the same topology but with very strong inter-chain bonds, forming a strong gel.

What we detected for Mebiol physical gels actually mirrors the effect of the quenching rate observed in simple glass-forming

liquids. For the latter, fast cooling can produce a "hyperquenched" glass at a "fictive" temperature $T_f$ where the structure of the liquid gets frozen that is much higher than the glass transition temperature $T_g$, conventionally defined in terms of the structural relaxation time. Conversely, a very slow cooling rate can produce a very stable glass with $T_f < T_g$, but still higher than the Kauzmann temperature $T_K$ where a thermodynamic phase transition to an "ideal" glass state with minimal configuration entropy is supposed to take place.[29] Compared to molecular glasses, polymer gels of course display an additional parameter to control the structural properties, namely, the polymer concentration.

Since we have seen that increasing $T$ does not necessarily yield a harder gel, the evidence we found rather suggests that fast quenching leads to a fictive *concentration* $c_f$ where gelation is observed (for fixed $T$) that is lower than the value found with adiabatic heating. One may also wonder whether the very existence of an "adiabatic" heating/cooling rate fixing a lowest attainable limit for $c_f$ does not imply that the gels that form in these conditions may be regarded as the counterpart of ideal glasses, namely, structures with a minimal amount of structural defects. Actually, the Mebiol gels generated by adiabatic heating display indeed negligible spatial heterogeneity and temporal aging.[13] Whether a comparable homogeneity and stability characterize rapidly quenched gels too is a subject of current investigation.

## SUPPLEMENTARY MATERIAL

See the supplementary material for the movies mentioned in the text.

## ACKNOWLEDGMENTS

We acknowledge funding from the Italian Ministry for Education, University and Research (PRIN Project No. 2017Z55KCW, "Soft Adaptive Networks").

## AUTHOR DECLARATIONS

### Conflict of Interest

The authors have no conflicts to disclose.

## DATA AVAILABILITY

The data that support the findings of this study are available from the corresponding author upon reasonable request.

## REFERENCES

[1] L. Klouda and A. G. Mikos, Eur. J. Pharm. Biopharm. **68**, 34 (2008).
[2] F. Tanaka, *Polymer Physics: Applications to Molecular Association and Thermoreversible Gelation* (Cambridge University Press, 2011).
[3] H. Yoshioka, M. Mikami, Y. Mori, and E. Tsuchida, J. Macromol. Sci., Part A: Pure Appl. Chem. **31**, 113 (1994).
[4] H. Yoshioka, M. Mikami, Y. Mori, and E. Tsuchida, J. Macromol. Sci., Part A: Pure Appl. Chem. **31**, 121 (1994).
[5] H. Yoshioka, S. Kubota, and Y. Mori, "Cell or tissue-culturing carrier, and culturing method," U.S. patent 6,897,064 (24 May 2005).
[6] Y. Lei and D. V. Schaffer, Proc. Natl. Acad. Sci. U. S. A. **110**, E5039 (2013).
[7] Q. Li, Q. Wang, O. Wang, K. Shao, H. Lin, and Y. Lei, PLoS One **13**, e0190364 (2018).
[8] E. Zaccarelli, J. Phys.: Condens. Matter **19**, 323101 (2007).
[9] E. Lattuada, D. Caprara, R. Piazza, and F. Sciortino, Sci. Adv. **7**, eabk2360 (2021).
[10] M. Formanek, L. Rovigatti, E. Zaccarelli, F. Sciortino, and A. J. Moreno, Macromolecules **54**, 6613 (2021).
[11] E. Secchi, T. Roversi, S. Buzzaccaro, L. Piazza, and R. Piazza, Soft Matter **9**, 3931 (2013).
[12] D. Larobina and L. Cipelletti, Soft Matter **9**, 10005 (2013).
[13] R. Piazza, M. Campello, S. Buzzaccaro, and F. Sciortino, Macromolecules **54**, 3897 (2021).
[14] T. G. Mason and D. A. Weitz, Phys. Rev. Lett. **74**, 1250 (1995).
[15] T. M. Squires and T. G. Mason, Annu. Rev. Fluid Mech. **42**, 413 (2010).
[16] V. Pelletier, N. Gal, P. Fournier, and M. L. Kilfoil, Phys. Rev. Lett. **102**, 188303 (2009).
[17] T. G. Mason, Rheol. Acta **39**, 371 (2000).
[18] M. Renaud, E. Mauret, and R. P. Chhabra, Can. J. Chem. Eng. **82**, 1066 (2004).
[19] Y. Almog and H. Brenner, Phys. Fluids **9**, 16 (1997).
[20] A. S. Khair and J. F. Brady, J. Fluid Mech. **557**, 73–117 (2006).
[21] T. Kalwarczyk, K. Sozanski, A. Ochab-Marcinek, J. Szymanski, M. Tabaka, S. Hou, and R. Holyst, Adv. Colloid Interface Sci. **223**, 55 (2015).
[22] Static and dynamic light scattering experiments confirm that Mebiol adsorbs on the probes, explaining the great stability of the PMMA particles in Mebiol solutions.
[23] At $T = 40\,^{\circ}\mathrm{C}$ $A' > A''$, suggesting that $G'$ may become larger than $G''$ for $\omega < 1$ Hz. However, we point out that all our measurements are performed for $\omega > 1$ Hz; therefore, extrapolation to lower frequency regimes has to be taken with care.
[24] Note that the gel phase defined according to the "rheological" criterion begins at temperatures that are substantially lower than the phase boundary in Fig. 1 obtained by a mechanical rigidity test.
[25] The power law fits in the low and high frequency regimes extend at least for a decade.
[26] G. C. Kalur, B. D. Frounfelker, B. H. Cipriano, A. I. Norman, and S. R. Raghavan, Langmuir **21**, 10998 (2005).
[27] G. Zhao, C. C. Khin, S. B. Chen, and B.-H. Chen, J. Phys. Chem. B **109**, 14198 (2005).
[28] S. C. Sharma, L. K. Shrestha, K. Tsuchiya, K. Sakai, H. Sakai, and M. Abe, J. Phys. Chem. B **113**, 3043 (2009).
[29] L. Berthier and G. Biroli, Rev. Mod. Phys. **83**, 587 (2011).